THE JOURNAL OF BIOLOGICAL CHEMISTRY VOL. 285, NO. 6, pp. 4122–4129, February 5, 2010

Two Pathways for Importing GDP-fucose into the Endoplasmic Reticulum Lumen Function Redundantly in the *O*-Fucosylation of Notch in *Drosophila*[*]

Received for publication, May 6, 2009, and in revised form, November 16, 2009 Published, JBC Papers in Press, November 30, 2009, DOI 10.1074/jbc.M109.016964

Hiroyuki O. Ishikawa[‡1], Tomonori Ayukawa[§1], Minoru Nakayama[‡], Shunsuke Higashi[§], Shin Kamiyama[¶], Shoko Nishihara[¶], Kazuhisa Aoki[‖], Nobuhiro Ishida[‖], Yutaka Sanai[‖], and Kenji Matsuno[‡§2]

From the [‡]Genome and Drug Research Center, Research Institute for Science and Technology, and the [§]Department of Biological Science and Technology, Tokyo University of Science, 2641 Yamazaki, Noda, Chiba 278-8510, the [¶]Department of Bioinformatics, Soka University, 1-236 Tangi-cho, Hachioji, Tokyo 192-8577, and the [‖]Department of Biochemical Cell Research, Tokyo Metropolitan Institute of Medical Science, 3-18-22 Honkomagome, Bunkyo-ku, Tokyo 113-8613, Japan

Notch is a transmembrane receptor that shares homology with proteins containing epidermal growth factor-like repeats and mediates the cell-cell interactions necessary for many cell fate decisions. In *Drosophila*, *O*-fucosyltransferase 1 catalyzes the *O*-fucosylation of these epidermal growth factor-like repeats. This *O*-fucose elongates, resulting in an *O*-linked tetrasaccharide that regulates the signaling activities of Notch. Fucosyltransferases utilize GDP-fucose, which is synthesized in the cytosol, but fucosylation occurs in the lumen of the endoplasmic reticulum (ER) and Golgi. Therefore, GDP-fucose uptake into the ER and Golgi is essential for fucosylation. However, although GDP-fucose biosynthesis is well understood, the mechanisms and intracellular routes of GDP-fucose transportation remain unclear. Our previous study on the *Drosophila* Golgi GDP-fucose transporter (Gfr), which specifically localizes to the Golgi, suggested that another GDP-fucose transporter(s) exists in *Drosophila*. Here, we identified Efr (ER GDP-fucose transporter), a GDP-fucose transporter that localizes specifically to the ER. Efr is a multifunctional nucleotide sugar transporter involved in the biosynthesis of heparan sulfate-glycosaminoglycan chains and the *O*-fucosylation of Notch. Comparison of the fucosylation defects in the *N*-glycans in *Gfr* and *Efr* mutants revealed that *Gfr* and *Efr* made distinct contributions to this modification; *Gfr* but not *Efr* was crucial for the fucosylation of *N*-glycans. We also found that *Gfr* and *Efr* function redundantly in the *O*-fucosylation of Notch, although they had different localizations and nucleotide sugar transportation specificities. These results indicate that two pathways for the nucleotide sugar supply, involving two nucleotide sugar transporters with distinct characteristics and distributions, contribute to the *O*-fucosylation of Notch.

Notch signaling is an evolutionarily conserved mechanism that regulates a broad spectrum of cell specification events through local cell-cell communication (1, 2). *Notch* encodes a single-pass transmembrane receptor protein with 36 epidermal growth factor (EGF)[3]-like repeats in its extracellular domain. Some of these EGF-like repeats, which contain a consensus sequence, are modified by the *O*-linked tetrasaccharide Sia-α2,3-Gal-β1,4-GlcNAc-β1,3-Fuc in mammals or the *O*-linked disaccharide GlcNAc-β1,3-Fuc in *Drosophila* (3, 4). In *Drosophila*, *O*-fucosyltransferase 1 catalyzes this *O*-linked fucosylation (5). *fringe* (*fng*) encodes another glycosyltransferase, β1,3 *N*-acetylglucosaminyltransferase, which adds GlcNAc specifically to the *O*-linked fucose of Notch and modulates the binding between Notch and its ligands (3, 6). The modulation of Notch activity through glycosylation by Fng family proteins is largely conserved between *Drosophila* and vertebrates (7). In contrast, the monosaccharide *O*-fucose modification of Notch is proposed to have no specific function except to provide a fucose moiety for further modification by Fng in *Drosophila* (8, 9).

Protein fucosylation requires GDP-fucose as a donor of fucose. Pathways for the synthesis of GDP-fucose are well understood (10, 11). Because fucosyltransferases in the Golgi utilize GDP-fucose, which is synthesized in the cytosol, as a fucose donor, the uptake of GDP-fucose into the Golgi is thought to be a critical step for fucosylation events. The GDP-fucose transporter is a nucleotide sugar transporter, classified as belonging to solute carrier family 35 (SLC35) (12). The transporter is predicted to span the Golgi membrane 10 times and couples the import of GDP-fucose into the Golgi lumen with the export of GMP into the cytoplasm; in the Golgi, GDP-fucose is used by specific fucosyltransferases to add fucose to a variety of glycoproteins and glycolipids. Recently, the gene responsible for congenital disorders of glycosylation (CDG) IIc was cloned by the complementation of cells derived from CDG IIc patients and was found to encode a GDP-fucose transporter, SLC35C1 (13, 14). CDG IIc, also termed leukocyte adhesion deficiency type II (LADII), is a rare recessive syndrome characterized by growth and mental retar-

[*] This work was supported by grants-in-aid from the Japanese Ministry of Education, Culture, Sports and Science (to K. M.) and grants from the Proposal-oriented Research Promotion Program, Japan Science and Technology Agency (to K. M.).

[1] Both authors contributed equally to this work.

[2] To whom correspondence should be addressed. Tel.: 81-4-7122-9714; Fax: 81-4-7125-1841; E-mail: matsuno@rs.noda.tus.ac.jp.

[3] The abbreviations used are: EGF, epidermal growth factor; AAL, *A. aurantia* lectin; CDG, congenital disorders of glycosylation; ER, endoplasmic reticulum; LADII, leukocyte adhesion deficiency type II; CFP, cyan fluorescent protein; GFP, green fluorescent protein; HA, hemagglutinin; HRP, horseradish peroxidase; HS-GAG, heparan sulfate-glycosaminoglycan.

dation and severe immunodeficiency with marked neutrophilia (15, 16).

Our previous study demonstrated that the *O*-fucosylation of Notch in *Drosophila* has a partial requirement for the *Drosophila* ortholog of SLC35C1, designated as Gfr (Golgi GDP-fucose transporter) (17). Furthermore, a mouse ortholog of SLC35C1 is required for mammalian Notch signaling *in vitro* (17). Based on these results, it was suggested that a reduction in Notch signaling could contribute to the pathology of CDG IIc/LADII (17). However, mutations of the *SLC35C1* genes in *Drosophila* and mouse yielded much more subtle phenotypes than those expected from the disruption of *fng* and its homologous gene functions (17, 18). These results suggested the existence of one or more additional GDP-fucose transporter genes in *Drosophila* and mammals. The identification of a novel GDP-fucose transporter and characterization of its function and intracellular distribution might help to elucidate the pathogenesis of CDG IIc/LADII. Here we describe a novel GDP-fucose transporter in *Drosophila* that localizes to the endoplasmic reticulum (ER) and participates in the *O*-fucosylation of Notch.

EXPERIMENTAL PROCEDURES

Drosophila Strains and Genetics—Flies were cultured in a standard medium at 25 °C unless otherwise stated. Canton-S was the wild-type line. *patched* (*ptc*)-*Gal4* and *engrailed* (*en*)-*Gal4* were used as Gal4 drivers. Cyan fluorescent protein-endoplasmic reticulum (CFP-ER) (BD Biosciences) and a green fluorescent protein (GFP) variant with an ER retention signal (KDEL) were used as ER markers. *UAS-fringe connection* (*frc*)-*N-Myc* (a gift from S. Goto), *UAS-Gfr-C-HA*, and *UAS-Gfr-C-Myc* were the UAS lines used (17). The Gfr^{1} and Gmd^{H78} mutants were described previously (17, 19).

To generate *Efr* (ER GDP-fucose transporter) mutants, *BG02156* (Bloomington Drosophila Stock Center, Indiana University, Bloomington, IN) was used as a starter P-element line. To excise the P-element, the *p*[Δ*2-3*] strain was used as a source of transposase. Mitotic clones were made in Efr^{1}, *FRT18A/Ubi-GFP*, *FRT18A*;; *MKRS, hs-flp*/+ larvae by Flp-mediated mitotic recombination. Recombination was induced in second instar larvae by a 30-min heat shock at 37 °C.

Construction of Plasmids—We amplified the Efr genome fragment from the presumed translation start codon to the stop codon (~1.0 kb) by genomic PCR and used it as the Efr cDNA, because Efr has no introns in its open reading frame (FBgn0029849). For UAS-Efr-N-HA and UAS-Efr-N-Myc, the hemagglutinin (HA) sequence tag and Myc epitope, respectively, were added to the 5′-end of the Efr cDNA by PCR. For UAS-$Efr^{\Delta KKVE}$-N-HA, the HA sequence tag was added to the 5′-end of the Efr cDNA as above, and the 3′-end of the Efr cDNA encoding its dilysine ER retention/retrieval signal (KKVE sequence) was deleted by PCR. pUAS-*Efr*-N-HA, pUAS-*Efr*-N-Myc, and pUAS-$Efr^{\Delta KKVE}$-N-HA were introduced into the *Drosophila* genome using a P-element-mediated transformation.

Nucleotide Sugar Transport Assay—*Efr* cDNA, tagged at the C terminus with HA, was subcloned into the copper-inducible expression vector pYEX-BX and introduced into the *Saccharomyces cerevisiae* strain YPH500. The *in vitro* nucleotide sugar transport assay was performed as described previously (17, 20).

Tissue Staining—Immunohistochemistry was performed according to standard protocols, except for the 3G10 antibody staining (see below) (21). The primary antibodies used were mouse anti-Wingless (Wg) (4D4, Developmental Studies Hybridoma Bank; 1:250), mouse anti-120-kDa integral Golgi membrane protein (7H6D7C2, EMD Biosciences; 1:500), mouse anti-Myc (9E10, Developmental Studies Hybridoma Bank; 1:1,000), rat anti-HA (3F10, Roche Applied Science; 1:1,000), rabbit anti- phosphorylated (activated) form of Mother against dpp (p-Mad) (PS1; 1:20,000) (22), and rabbit anti-GFP (MBL, 1:1,000). The secondary antibodies were Alexa Fluor 488-conjugated goat anti-rabbit IgG (Invitrogen; 1:500), Alexa Fluor 488-conjugated goat anti-mouse IgG (Invitrogen; 1:500), cyanine 3-conjugated donkey anti-mouse IgG (Rockland; 1:500), cyanine 3-conjugated goat anti-rat IgG (Rockland; 1:500), cyanine 5-conjugated goat anti-rat IgG (Rockland, 1:500), and cyanine 5-conjugated donkey anti-rat IgG (Invitrogen; 1:500).

To detect HS-GAG chains, staining with the 3G10 antibody (Seikagaku, Tokyo, Japan) was performed as described previously (23). Biotin-conjugated ALL (1 μg/ml) (Seikagaku, Tokyo, Japan) and Streptavidin-conjugated Alexa 555 (Invitrogen, 1:500) were used for the *Aleuria aurantia* lectin (AAL) staining. All images were obtained by confocal microscopy (Pascal, Zeiss).

Western Blotting Analysis—For Western blotting analyses, a rat anti-HA antibody (3F10, Roche Applied Science; 1:500), a rabbit anti-horseradish peroxidase (HRP) antibody (Cappel; 1:12,500), an HRP-conjugated goat anti-rat antibody (KPL Europe; 1:2,000), an HRP-conjugated goat anti-rabbit antibody (1:2,000; Open Biosystems), and enhanced chemiluminescence reagents (GE Healthcare) were used.

RESULTS

Drosophila Efr Encodes Another GDP-fucose Transporter—The *Drosophila CG3774* gene has been identified as a putative ortholog of human *SLC35B4*, which encodes a UDP-GlcNAc/UDP-xylose transporter (24). However, a *Caenorhabditis elegans* SLC35B4 homolog was reported to have some GDP-fucose transport activity (13, 14). Thus, we first tested whether *Drosophila* CG3774 could transport GDP-fucose. We examined the biochemical activity of CG3774 for transporting various nucleotide sugars, using a yeast *in vitro* system (20). Microsomes were prepared from transformants carrying vectors with and without a *CG3774* cDNA insert, and their ability to transport nucleotide sugars was investigated (Fig. 1*A*). We found that CG3774 transport of GDP-fucose, UDP-GlcNAc, and UDP-xylose was more than 1.5 times that of control samples, and CG3774 did not transport CMP-sialic acid, UDP-glucuronic acid, GDP-mannose, or UDP-glucose (Fig. 1*A*). On the other hand, the transport of UDP-galactose and UDP-*N*-acetylgalactosamine was reduced by the expression of *CG3774* (Fig. 1A). This suppression could be explained by possible dimerization between CG3774 and endogenous nucleotide sugar transporters (25, 26), which could lead to inhibition of the activity of the latter, as reported before in similar

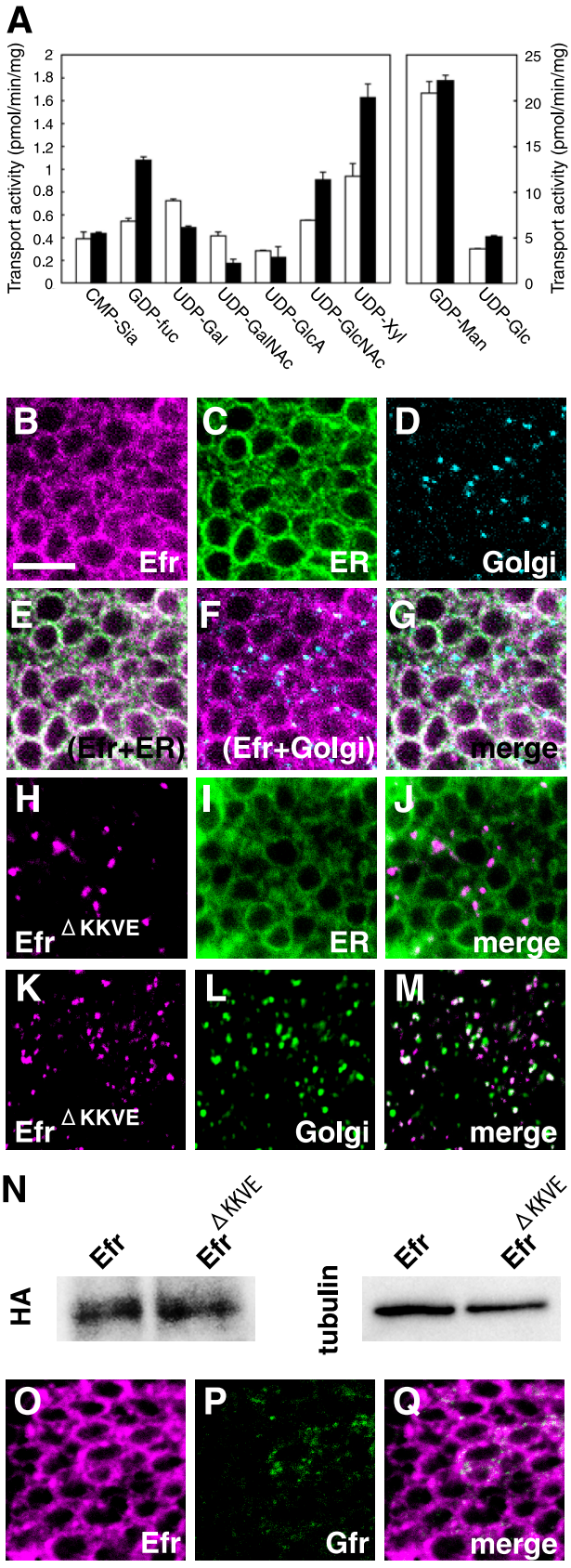

FIGURE 1. **The *Drosophila* homolog of SLC35B4, Efr, transported GDP-fucose, UDP-*N*-acetylglucosamine, and UDP-xylose and was specifically localized to the ER.** *A*, the transport of CMP-sialic acid (*CMP-Sia*), GDP-fucose (*GDP-Fuc*), UDP-Gal, UDP-GalNAc, UDP-GlcA, UDP-GlcNAc, UDP-xylose (*UPD-Xyl*), GDP-mannose (*GDP-Man*), and UDP-Glc into vesicles prepared from *S. cerevisiae* expressing *Drosophila* SLC35B4 from transfected pYEX-BX-*Efr*-C-HA (*solid bars*) or from the mock-transfected equivalent (*open bars*). Values are the mean ± S.E. from duplicate experiments. *B–G*, subcellular localization of HA-tagged *Drosophila* CG3774 (Efr-N-HA) in the epithelium of third instar wing discs. *UAS-Efr-N-HA* and *UAS-CFP-ER* were driven by *ptc-Gal4*. Efr (*magenta* in *B*, *E*, *F*, and *G*), CFP-ER (ER) (*green* in *C*, *E*, and *G*), and Golgi (*cyan* in *D*, *F*, and *G*) were detected by triple staining with anti-HA, anti-GFP, and anti-Golgi 120-kDa protein antibodies, respectively. *E–G* are merged images of *B* and *C*; *B* and *D*; and *B*, *C*, and *D*, respectively. *H–M*, subcellular localization of HA-tagged *Drosophila* CG3774 derivative lacking its dilysine ER retention/retrieval signals (Efr$^{\Delta KKVE}$-N-HA) in the epithelium of third instar wing discs. *UAS-Efr*$^{\Delta KKVE}$*-N-HA* and *UAS-CFP-ER* were driven by *ptc-Gal4*. Efr$^{\Delta KKVE}$ (*magenta* in *H*, *J*, *K*, and *M*) and CFP-ER (*green* in *I* and *J*) or Golgi (*green* in *L* and *M*) were detected by double staining with anti-HA and anti-GFP or anti-Golgi 120-kDa protein antibodies, respectively. *J* and *M* are *merged images* of *H* plus *I* and *K* plus *L*, respectively. *N*, a Western blot analysis of Efr-N-HA and Efr$^{\Delta KKVE}$-N-HA proteins. *UAS-Efr-N-HA and UAS-Efr*$^{\Delta KKVE}$*-N-HA* were driven by *da-Gal4*, and whole protein extracts were prepared from the embryos. These samples were analyzed by a Western blot using anti-HA antibody (*HA*). For an internal control, anti-β-tublin antibody (*tublin*) was used. *O–Q*, subcellular localization of Myc-tagged *Drosophila* CG3774 (Efr-N-Myc) and Gfr-C-HA in the epithelium of third instar wing discs. *UAS-Efr-N-Myc* and *UAS-Gfr-C-HA* were driven by *ptc-Gal4*, and Efr (*magenta* in *O* and *Q*) and Gfr (*green* in *P* and *Q*) were detected by double staining with anti-Myc and anti-HA antibodies, respectively. *Q* is a *merged image* of *O* and *P*. *Bar*, 5 μm.

situations (26, 27). Similarly, it is possible that the increase of GDP-fucose, UDP-GlcNAc, and UDP-xylose transport is due to the activation of endogenous nucleotide sugar transporters via this possible dimerization with CG3774. However, our genetic analyses below supported the idea that CG3774 indeed contributes to the transport of these nucleotide sugars in *Drosophila*.

The deduced *Drosophila* SLC35B4 protein is composed of 352 amino acids with 10 putative transmembrane domains and dilysine ER retention/retrieval signals (KK*XX* or K*X*K*XX*). As expected, therefore, we found that CG3774-N-HA co-localized with an ER marker, CFP-ER (Fig. 1, *B–D*) but not with a generic Golgi marker, the Golgi 120-kDa protein, in wing disc cells (Fig. 1, *E–G*). CG3774 was predominantly localized to the ER; therefore, we called it Efr (for "ER GDP-fucose transporter"). To exclude the possibility that the localization of Efr to the ER is due to the mislocalization of this protein caused by its overexpression, we also examined the subcellular localization of an Efr derivative (Efr$^{\Delta KKVE}$), lacking its putative dilysine ER retention/retrieval signal (KKVE). Under the same conditions, Efr$^{\Delta KKVE}$ failed to localize to the ER (Fig. 1, *H–J*) but was detected in the Golgi (Fig. 1, *K–M*). In addition, a Western blot analysis revealed that almost equal amounts of Efr and Efr$^{\Delta KKVE}$ proteins were produced from *UAS-Efr-N-HA* and *UAS-Efr*$^{\Delta KKVE}$*-N-HA*-driven embryos, suggesting that the distinct subcellular localization of these proteins was not due to the difference in their expression level (Fig. 1*N*).

These results confirm that Efr is an ER-resident protein, and its dilysine ER retention/retrieval signal localizes Efr to the ER. The localization of Efr did not overlap with that of a previously identified GDP-fucose transporter, Gfr, which specifically localizes to the Golgi (Fig. 1, *O–Q*).

HS-GAGs Synthesis Partly Requires Efr—Next, to understand the roles of *Efr*, we generated mutations of *Efr* in *Drosophila*. We used an approach involving imprecise excision of a P-element, a *Drosophila* transposon. Derivative strains that lost the P-element were established from *BG02156*, in which the P-element was inserted at the 5′-end of the *Efr* gene locus (Fig. 2*A*).

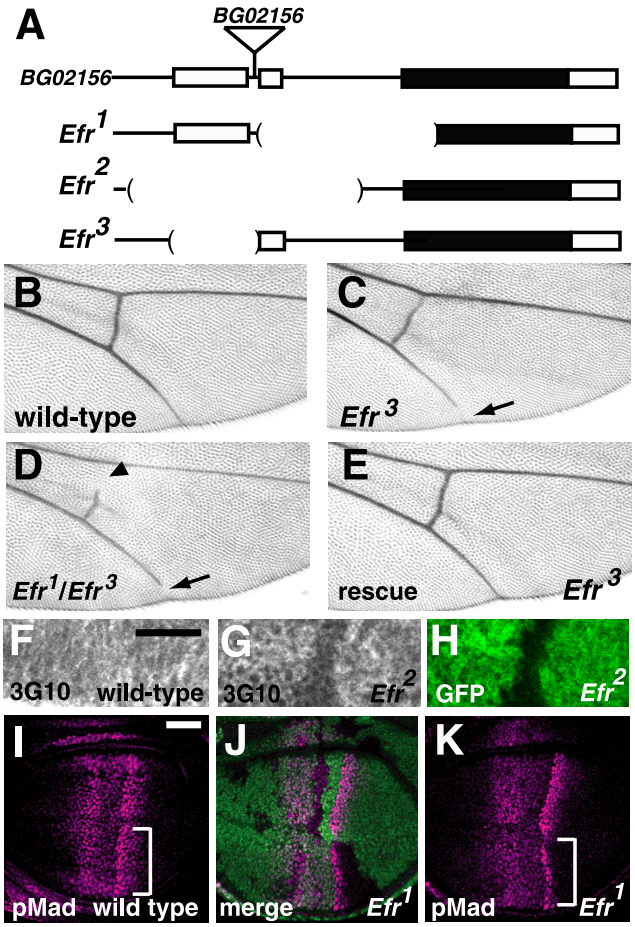

FIGURE 2. ***Efr* was involved in HS-GAG biosynthesis *in vivo*.** *A*, genomic organization of the *Efr* locus. The exons of the *Efr* gene are shown as *boxes*, and the predicted coding regions are *filled* in *black*. The genomic regions deleted in the Efr^1, Efr^2, and Efr^3 mutants are indicated by *parentheses*. In the Efr^1 mutant, a ~1.2-kb genomic region that includes a predicted initiation codon, was deleted. In the Efr^2 mutant, a ~1.5-kb genomic region that includes the first and second exons was deleted. In the Efr^3 mutant, a ~0.5-kb genomic region that includes the first exon was deleted. *BG02156* was the original P-element insertion line, and a *triangle* indicates the position of the P-element insertion site. *B–E*, adult wings. *B*, a wild-type wing. *C* and *D*, a wing of Efr^3/Efr^3 (*C*) and a wing of Efr^3/Efr^3 (*D*), demonstrating the gap in the fifth longitudinal vein (*arrow*). In *D*, a gap in the posterior cross-vein was also observed (*arrowhead*). *E*, a wing of Efr^3/Efr^1 carrying a transgene of the *Efr* genome fragment. The wing vein gap was completely rescued. *F–H*, anti-heparan sulfate (3G10) staining of the late third instar wing discs. *F*, a wild-type wing disc. *G* and *H*, a chimeric wing disc, including Efr^2/Efr^2 cells, which are marked by the absence of GFP (*H*). Note that the intensity of anti-heparan sulfate staining was reduced in the mutant cells (*G*). *I–K*, late third instar wing discs stained with an anti-p-Mad antibody (*magenta*). *I*, a wild-type wing disc. *J* and *K*, a chimeric wing disc, including Efr^1/Efr^1 cells, which are marked by the absence of GFP (*green* in *J*). Anti-p-Mad antibody staining was decreased in Efr^1 mutant cells (regions indicated by *brackets* in *I* compared with that of *K*). *Bar*, 25 μm.

The genomic lesions were identified by PCR and genomic sequence analyses, and we obtained three deletion lines, designated Efr^1, Efr^2, and Efr^3 (Fig. 2*A*). In Efr^1, the second exon, second intron, and the 5′ region of the third exon, which includes the predicted initiation codon, were deleted, suggesting that Efr^1 was a null allele of *Efr* (Fig. 2*A*). In Efr^2, the first and second exons and the first and most of the second introns were deleted (Fig. 2*A*). Homozygotes and hemizygotes of Efr^1 or Efr^2 were lethal, although some of them survived until the third-instar larval stage (24% of Efr^1 and 30% of Efr^2 homozygotes). This is possibly due to maternally supplied *Efr* mRNA, which was detected by *in situ* hybridization (data not shown). Introduction of a genomic fragment of the *Efr* locus into the genome rescued this lethality (data not shown). In Efr^3, the first exon was deleted (Fig. 2*A*). In the adult wings of the Efr^3 homozygotes and hemizygotes, a gap in the fifth longitudinal vein was observed (Fig. 2*C*) (data not shown). In Efr^3/Efr^1, this phenotype became more severe than in the homozygous Efr^3, and a gap in the posterior cross-vein was also observed (Fig. 2*D*). The phenotype of the Efr^3 homozygote was completely rescued by introducing a genomic fragment of the *Efr* locus, indicating that this phenotype was caused by the loss of *Efr* gene functions (Fig. 2*E*). This phenotype is reminiscent of that of *Dally* hypomorphic mutants (28). *Dally* encodes the core protein of *Drosophila* glypican, an HS-GAG proteoglycan (28).

As demonstrated above, Efr transports UDP-GlcNAc and UDP-xylose, which are required for HS-GAG biosynthesis. In addition, the presence of the wing phenotype that is similar to that of *Dally* could be due to a defect in HS-GAG synthesis. Therefore, we examined the effect of the *Efr* mutation on the biosynthesis of HS-GAG chains. The wing discs of third instar larvae were stained with the monoclonal antibody 3G10, which recognizes an epitope produced by heparitinase I digestion of HS-GAG chains (29). In the wild-type wing discs, uniform 3G10 antibody staining was detected (Fig. 2*F*). However, in somatic clones of the Efr^2 mutant (marked by the lack of GFP in Fig. 2*H*) induced by the FLP/FRT system, the 3G10 staining was slightly reduced (Fig. 2, *G* and *H*). These results suggest that the biosynthesis of HS-GAGs partly requires an *Efr* function in *Drosophila*.

HS-GAGs play important roles in the functions of various morphogens, such as Dpp (Decapentaplegic), Hh (Hedgehog), and Wg (Wingless) (30, 31). Thus, we investigated the functions of *Efr* in these morphogen-mediated signaling pathways. First, we detected the activation of Dpp signaling by antibody staining for p-Mad, a cytoplasmic signal transducer of Dpp signaling (32). In the wild-type wing disc, the p-Mad level was high in the central region of the wing pouch, because *dpp* is expressed in a stripe of the anterior compartment along the anterior-posterior compartment boundary (Fig. 2*I*). However, as shown in Fig. 2, *J* and *K*, the p-Mad level was decreased in the *Efr* mutant cells. This phenotype was similar to that of mutants for genes required for the synthesis of HS-GAGs, which play important roles in the functions of Dpp (23, 33, 34). Therefore, these results suggest that Dpp signaling in the wing disc partly requires *Efr* function. In contrast, the mutation of *Gfr* does not affect HS-GAG synthesis or Dpp signaling (17), indicating that Efr and Gfr have distinct activities, at least in part. We also examined the effect of the *Efr* mutant in Hh and Wg signaling; however, neither was affected in the *Efr* mutant (data not shown).

In Combination with Gfr, Efr Has an Essential Role in Notch Signaling—We previously reported that the *O*-fucosylation of Notch has a partial requirement for *Gfr*, suggesting that at least one other GDP-fucose transporter is present in *Drosophila* (17). Given that Efr transported GDP-fucose *in vitro*, we speculated that *Efr* function might be involved in the *O*-fucosylation of Notch. In wild-type wing discs, Notch signaling is activated

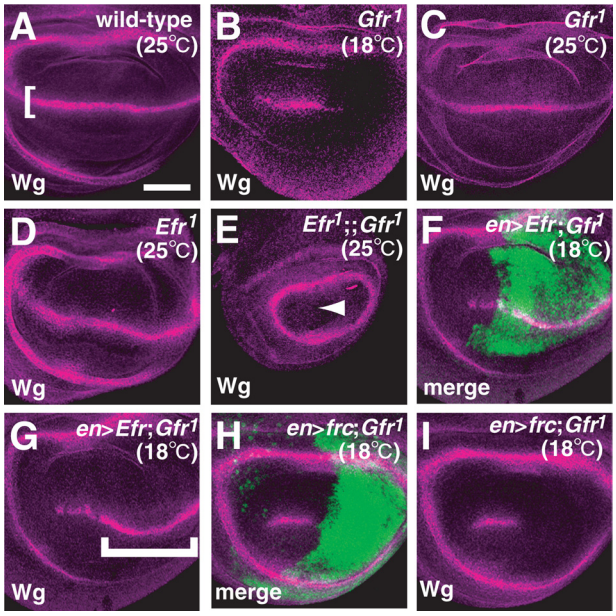

FIGURE 3. ***Efr* and *Gfr* functioned redundantly in Notch signaling.** *A–I*, anti-Wg antibody staining (*magenta*) of late third instar wing discs. *A*, a wild-type wing disc. The Notch signaling-dependent expression of *wg* along the dorsal-ventral compartment boundary is indicated by a *bracket*. *B*, a wing disc of Gfr^1/Gfr^1 at 18 °C. *C*, a wing disc of Gfr^1/Gfr^1 at 25 °C. *D*, a wing disc of Efr^1/Y at 25 °C. *E*, a wing disc of Efr^1/Y;;Gfr^1/Gfr^1 at 25 °C. The Notch signaling-dependent expression of *wg* was completely abolished (*arrowhead*). *F* and *G*, a wing disc of Gfr^1/Gfr^1-overexpressing *Efr* under the control of *en*-Gal4 at 18 °C. *F*, anti-GFP antibody staining (*green*) shows the region overexpressing *Efr*. *G*, the Notch signaling-dependent expression of *wg* was restored in the region expressing *Efr* (*bracket*). *H* and *I*, a wing disc of Gfr^1/Gfr^1 overexpressing *frc* under the control of *en*-Gal4 at 18 °C. *H*, anti-GFP antibody staining (*green*) shows the region overexpressing *frc*. *I*, the Notch signaling-dependent expression of *wg* was not restored. *Bar*, 50 μm.

and induces *wg*, a target gene of Notch signaling, along the dorsal-ventral compartment boundary in the late third instar (Fig. 3*A*) (35, 36). *wg* induction depends on the modulation of Notch ligand binding by Fng, which adds GlcNAc to *O*-fucose on the EGF-like repeats of Notch (3, 6). Therefore, the *O*-fucosylation of these EGF-like repeats is also essential for *wg* induction. As reported previously, in the wing disc of Gfr^1 (a null allele) homozygotes, the expression of *wg* was partially reduced at the non-permissive temperature (18 °C) (Fig. 3*B*), but this defect was not observed at the permissive temperature (25 °C) (Fig. 3*C*) (17). However, *wg* expression was not affected in Efr^1 or Efr^2 homozygous wing discs at either 18 or 25 °C (Fig. 3*D*) (data not shown). Therefore, we next tested whether *Efr* and *Gfr* function redundantly as GDP-fucose transporters, by examining a double mutant of *Efr* and *Gfr*. In the double mutant wing discs of Efr^1 and Gfr^1 or Efr^2 and Gfr^1, the Notch signaling-dependent *wg* expression was completely abolished at the dorsal-ventral boundary at 25 °C (Fig. 3*E*) (data not shown). This phenotype is similar to that of wing discs homozygous for *Gmd* (GDP-mannose-4,6-dehydratase), which is essential for GDP-fucose synthesis in *Drosophila* (8, 19), or homozygous for *O*-fucosyltransferase 1 (5, 37).

If *Efr* acts as a GDP-fucose transporter, the overexpression of *Efr* should rescue the reduced Notch signaling activity in the wing disc of the *Gfr* homozygote at the non-permissive temperature (18 °C). In the posterior compartment of wing discs homozygous for Gfr^1, *Efr* was overexpressed by *en-Gal4*. This restored the expression of *wg* at 18 °C in all cases examined ($n = 15$) (Fig. 3, compare *F* and *G* with *B*). On the other hand, the overexpression of *frc*, which encodes a transporter capable of transporting various UDP-sugars, including UDP-GlcNAc and UDP-xylose, but not GDP-fucose, failed to rescue this *wg* expression under the same conditions in all cases examined ($n = 15$) (Fig. 3, *H* and *I*). This result suggests that the incorporation of GDP-fucose, but not of UDP-GlcNAc or UDP-xylose, is responsible for the rescue of Notch signaling activity, although Efr also transports these other two nucleotide sugars, as described above.

It was recently found that *rumi*, which encodes an *O*-glucose transferase, is essential for Notch signaling in *Drosophila* (38). Rumi adds *O*-glucose to a subset of Notch EGF-like repeats, and two xylose moieties are further added to this *O*-glucose (38). However, Efr and Gfr do not transport UDP-glucose (17). Therefore, it is unlikely that the reduction of Notch signaling in the *Gfr* mutant is associated with a defect in the *O*-glucosylation. In addition, the xylose elongation is probably not involved in the rescue of Notch signaling by the overexpression of *Efr* in *Gfr* homozygotes either, because Frc, which transports UDP-xylose *in vitro*, did not rescue the Notch signaling activity in the *Gfr* homozygote, as mentioned above. Consistent with this idea, in wing discs double homozygous for $rumi^{44}$, a null mutation of *rumi*, and either Efr^1 or Gfr^1, the expression of *wg* was not reduced further than in the *Efr* or *Gfr* homozygotes at 18 °C (data not shown).

Gfr but Not Efr Plays a Major Role in the Fucosylation of N-Glycans—AAL is defined as an L-fucose lectin that recognizes α-1,3- and α-1,6-linked fucose residues (39, 40). In the wild-type wing discs of third instar larvae, AAL staining was ubiquitously detected (Fig. 4*A*). However, as reported previously, in Gfr^1 homozygous wing discs, AAL staining was virtually abolished (Fig. 4*B*) (17). In contrast, in the wing discs homozygous for Efr^1 or Efr^2, this staining was not affected under the same conditions (Fig. 4*C*) (data not shown). Furthermore, the reduced AAL staining in the Gfr^1 mutant wing discs was not restored by the overexpression of *Efr* driven by *en-Gal4* (Fig. 4, *D–F*) (data not shown), although a similar overexpression of *Gfr* does restore the AAL staining in Gfr^1 mutant wing discs (17). Therefore, unlike *Gfr*, *Efr* did not play a role in the fucose modifications of *N*-glycans.

We next confirmed the influence of the *Efr* and *Gfr* mutations on the fucose modifications of bulk proteins by a biochemical approach. The imaginal discs and central nervous system were isolated from wild-type, Efr^1/Efr^1, Gfr^1/Gfr^1, the double homozygote of Efr^1 and Gfr^1, and Gmd^{H78}/Gmd^{H78} third instar larvae cultured at 25 °C. The protein extracts of these organs were then analyzed by Western blotting with an anti-HRP antibody, which recognizes the α-1,3-fucose (41). Consistent with the above results obtained by tissue staining with AAL, the Western blot analysis showed that the reactivity of the anti-HRP antibody was not affected in the lysate of the Efr^1 mutant (Fig. 4*G*, *Efr^1 lane*). In contrast, this reactivity was significantly reduced in the lysate of the Gfr^1 mutant (Fig. 4*G*, *Gfr^1 lane*). The reactivity in the lysate of the Efr^1 and Gfr^1 double homozygote was not reduced further (Fig. 4*G*, *Efr^1;Gfr^1 lane*), although the Notch signaling activity was diminished in

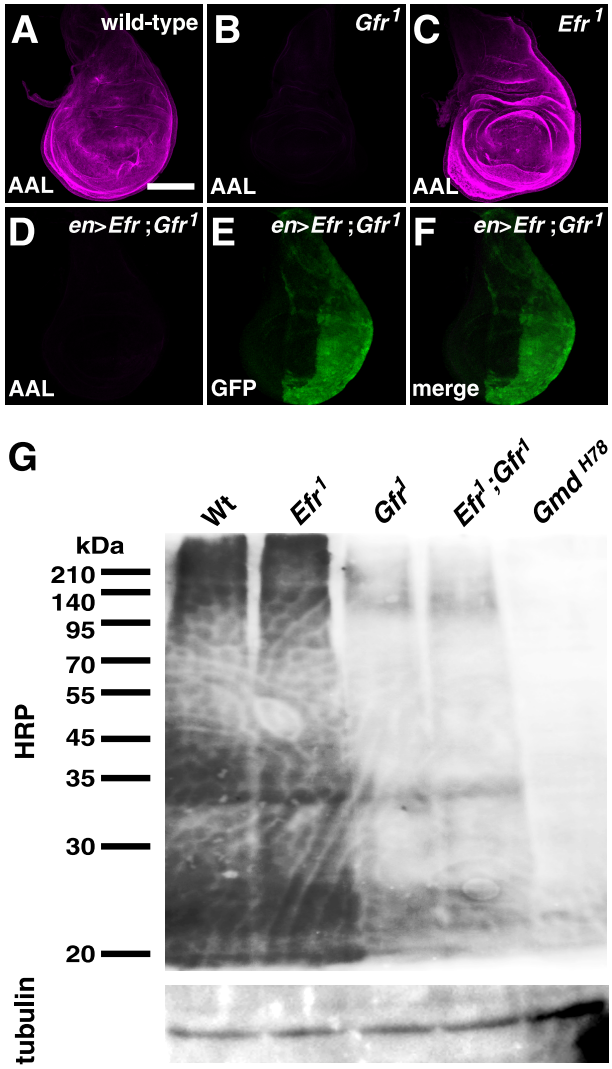

FIGURE 4. ***Gfr* but not *Efr* was required for fucose modifications of *N*-glycans.** *A–C*, AAL staining (*magenta*) of the late third instar wing discs. *A*, a wild-type wing disc. *B*, a wing disc of Gfr^1/Gfr^1. *C*, a wing disc of Efr^1/Y. All confocal images were obtained under the same conditions. *D–F*, a wing disc of Gfr^1/Gfr^1 overexpressing *Efr* under the control of *en-Gal4*. *D*, AAL staining (*magenta*). *E*, anti-GFP antibody staining (*green*) showing the region overexpressing *Efr*. *F*, a *merged image* of *D* and *E*. *G*, Western blot analysis of the total protein extracts prepared from the imaginal discs and central nervous system of wild-type (*Wt*), Efr^1/Y (Efr^1), Gfr^1/Gfr^1 (Gfr^1), Efr^1/Y;; Gfr^1/Gfr^1 (Efr^1; Gfr^1), and Gmd^{H78}/Gmd^{H78} (Gmd^{H78}) mutant larvae. α-1,3-fucose modifications were detected by anti-HRP antibody staining. *Bar*, 100 μm.

this double homozygote compared with the single homozygotes of either of these mutants under the same conditions. Based on these results, we concluded that *Efr* does not play a crucial role in the fucosylation of *N*-glycans. These results are consistent with a previous finding that the disruption of *N*-glycan fucosylations does not disrupt Notch signaling activity, further suggesting that these fucose modifications do not play a crucial role in Notch signaling (17). On the other hand, in the lysate of the Gmd^{H78} mutant, in which GDP-fucose is not synthesized, the reactivity to the anti-HRP antibody was abolished (Fig. 4*G*, Gmd^{H78} *lane*). Thus, there is a weak, residual *N*-glycan fucosylation activity in the double homozygote of Efr^1 and Gfr^1. This finding suggests the existence of a third GDP-fucose transporter in *Drosophila*.

Efr and Gfr Have Redundant Roles That Are Essential for the O-Fucosylation of Notch—In contrast to the fucosylation of *N*-glycans, it is difficult to examine the level of protein *O*-fucosylation directly. Therefore, we used an indirect approach, involving the ectopic expression of *fng*, to determine whether *Efr* is required for the *O*-fucosylation of Notch. The regions expressing GFP indicate where *fng* is expressed under the control of *ptc-Gal4*. As reported previously, the ectopic expression of *fng* driven by *ptc-GAL4* resulted in an ectopic induction of *wg* in a stripe posterior to the region ectopically expressing *fng* in the ventral compartment of the wild-type wing disc at the third instar (Fig. 5, *A–C*) (3, 6). The functions of *fng* depend on the *O*-fucosylation of Notch; therefore, the absence of Notch *O*-fucosylation should prevent this ectopic *wg* induction by *fng*. We previously demonstrated that the ectopic expression of *fng* induces a normal level of *wg* expression in the wing discs of Gfr^1 homozygotes at the permissive temperature (25 °C) (Fig. 5, *D–F*) (17). In the wing discs of *Efr* homozygotes, the ectopic induction of *wg* by *fng* overexpression was also not affected at 25 °C (Fig. 5, *G–I*). In contrast, in all wing discs isolated from double homozygotes of Efr^1 and Gfr^1 at the same stage and temperature ($n = 17$), the ectopic expression of *fng* did not induce *wg*. This suggests that Notch *O*-fucosylation was absent in these wing discs (Fig. 5, *J–L*). This phenotype was essentially the same as that induced by *fng* expression in the wing discs of Gmd^{H78} homozygotes under the same conditions ($n = 19$) (Fig. 5, *M–O*). Therefore, *Efr* and *Gfr* have redundant roles, which are essential for the *O*-fucosylation of Notch.

DISCUSSION

Nucleotide sugars are transported into the ER and Golgi, where they become donors of saccharides for the enzymatic reactions of various glycosyltransferases. The properties of several nucleotide sugar transporters, which transport overlapping species of nucleotide sugars, have been studied in detail. Many of these transporters are distributed in the ER and Golgi. The intracellular routes for the nucleotide sugar supplies are not well understood, and they are predicted to be very complex. In this study, we identified two pathways in *Drosophila* for transporting GDP-fucose into the ER, where the *O*-fucosylation of Notch occurs.

We identified Efr as a second GDP-fucose transporter in *Drosophila* and demonstrated that *Gfr* and *Efr* have redundant roles for the *O*-fucosylation of Notch. Despite the similar roles of *Gfr* and *Efr* in *O*-fucosylation, these two nucleotide sugar transporters have distinct biochemical and cell biological characteristics. First, the specificities of the transported nucleotide sugars are quite different between them. Efr transports a broader spectrum of nucleotide sugars than Gfr, including UDP-GlcNAc, UDP-xylose, and GDP-fucose. Thus, *Efr* simultaneously contributes to HS-GAG synthesis and the *O*-fucosylation of Notch. In contrast, Gfr transports GDP-fucose almost exclusively (17). Therefore, in the *Gfr* homozygotes, HS-GAG synthesis was not affected, whereas the fucosylation of bulk protein *N*-glycans was mostly abolished. Second, the subcellular localizations of Efr and Gfr are different; they are specifically localized to the ER and Golgi, respectively. These results together with the previous finding that *O*-fucosylation occurs

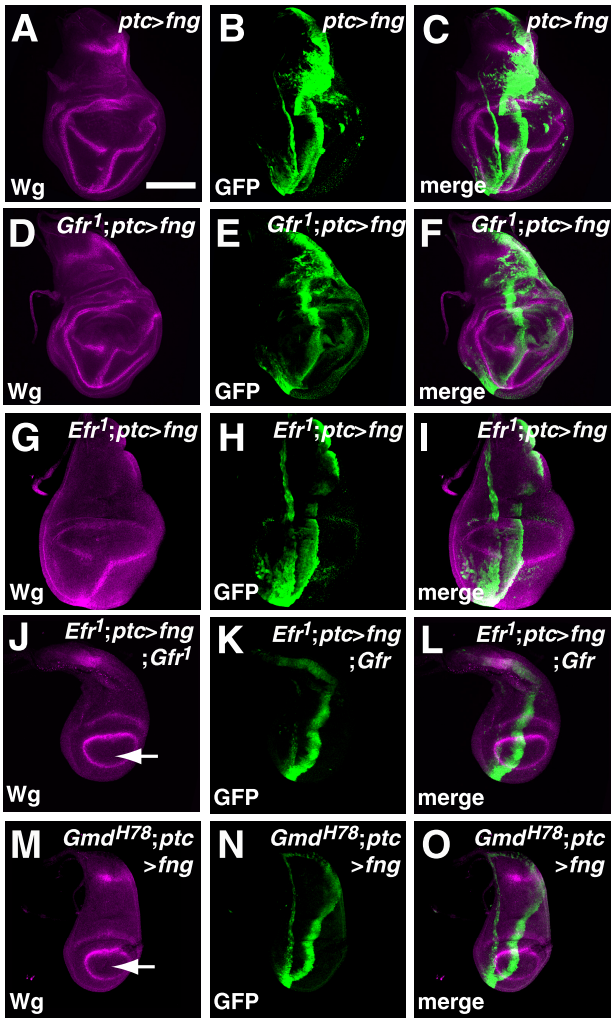

FIGURE 5. ***Efr* and *Gfr* function redundantly for the *O*-fucosylation of Notch.** *A–O*, the expression of *wg* (*magenta* in *A*, *C*, *D*, *F*, *G*, *I*, *J*, *L*, *M*, and *O*) in wild-type or various mutant wing discs of late third-instar larvae that ectopically express *fng* and *GFP* (*green* in *B*, *C*, *E*, *F*, *H*, *I*, *K*, *L*, *N*, and *O*). The expression of *fng* and *GFP* was driven by *ptc-Gal4*. *A–C*, a wild-type wing disc; *D–F*, Gfr^1/Gfr^1; *G–I*, Efr^1/Y; *J–L*, $Efr^1/Y;;Gfr^1/Gfr^1$; *M–O*, Gmd^{H78}/Gmd^{H78}. GFP shows the regions ectopically expressing *fng*. *J* and *M* show the ectopic expression of *fng* failed to induce ectopic *wg* expression (*arrows*). *C*, *F*, *I*, *L*, and *O* are *merged images* of *A* and *B*, *D* and *E*, *G* and *H*, *J* and *K*, and *M* and *N*, respectively. *P*, two pathways for transporting GDP-fucose to the ER, where the *O*-fucosylation of Notch occurs in *Drosophila*. GDP-mannose-4,6-dehydratase (*Gmd*) and GDP-4-keto-6-deoxymannose epimerase/reductase (*FX*) convert GDP-fucose from GDP-mannose in the cytoplasm (*arrows* at *left*). GDP-fucose is then transported into the ER or Golgi by two GDP-fucose transporters, Efr and Gfr, respectively. GDP-fucose is incorporated by Gfr into the Golgi, where it is used for the fucosylation of *N*-glycans. GDP-fucose that is incorporated into the Golgi by Gfr is also transported to the ER, possibly by retrograde vesicular transport. In the ER, where the *O*-fucosylation of Notch occurs, GDP-fucose is used as a donor of fucose for this modification of Notch. *Bar*, 100 μm.

in the ER (42) indicate that GDP-fucose is supplied from two pathways, one in the ER and one in the Golgi, as shown schematically in Fig. 5*P*. This is the first example of such a dual system for supplying a nucleotide sugar to the ER for a specific glycosylation. In the first pathway, GDP-fucose is directly incorporated into the ER via Efr, although Efr is involved in the incorporation of various nucleotide sugars (Fig. 5*P*). In the second pathway, GDP-fucose is incorporated into the Golgi via Gfr and transported into the ER, where the *O*-fucosylation of Notch takes place, possibly via retrograde vesicular trafficking from the Golgi to the ER (Fig. 5*P*).

Recent studies have demonstrated that the substrate specificities of nucleotide sugar transporters are very difficult to predict based on their primary structure (25). We generated a null mutant of *Drosophila CG14971*, an ortholog of mouse *Slc35c2* whose primary structure is most closely related to *Drosophila Gfr*. However, our genetic analysis of this mutant did not provide any indication that it plays a role in fucose modifications (data not shown). On the other hand, although the sequence identity of Efr and Gfr is only 10%, both of these nucleotide sugar transporters transport GDP-fucose for the catalytic activity of *O*-fucosyltransferase 1. Thus, our results provide another example of the difficulty of predicting the substrate specificity of nucleotide sugar transporters. Our results also suggest that collaborative functions of nucleotide sugar transporters that belong to distantly related groups need to be considered to elucidate their redundant roles.

In the mouse, *Slc35c1*, the ortholog of *Gfr*, plays a crucial role in fucose modifications *in vivo* (18). Thus, mice homozygous for a *Slc35c1*-null mutation show hypofucosylation of glycoproteins, the absence of selectin ligands, growth retardation, and postnatal defects in various organs (18, 43). However, these defects are significantly less severe than those associated with the mutation of *FX*, which encodes an enzyme that converts GDP-mannose to GDP-fucose, although some of the defects overlap (44). This observation suggests the presence of another GDP-fucose transporter in the mouse. This idea is also supported by the observation that the hypofucosylation in *Slc35c1* mutant cells is restored by adding fucose, indicating the presence of a residual activity for GDP-fucose incorporation (18). Furthermore, the oral administration of fucose is an effective therapy for the immunodeficiency of CDG IIc patients, which have mutations in their SLC35C1 locus (45, 46). In cultured fibroblasts from a CDG IIc patient, fucosylation of *N*-glycans is significantly reduced, whereas *O*-fucosylation of Notch is not affected (47). This result also suggests the presence of additional GDP-fucose transporters that provide a sufficient level of GDP-fucose for the *O*-fucosylation of Notch in the absence of SLC35C1 in human. The residual activities of GDP-fucose incorporation in the absence of SLC35C1 or its ortholog (Gfr) could be more predominant in human than *Drosophila*, because the *O*-fucosylation of Notch was affected in *Drosophila*

but not in human under this condition. However, this comparison is based on experiments involving very different systems, and there might be other explanations (17). Taken together, these observations suggest that at least one other GDP-fucose transporter is also present in mammals. In this study, we revealed the nature of this redundancy in *Drosophila*, which could be important for understanding how a low level of GDP-fucose transporting activity is maintained in CDG IIc patients.

Acknowledgments—We thank Y. Takei-Yamaguchi, T. Tabata, M. Kawakita, N. Taniguchi, and Y. Nagai for valuable suggestions. We also thank the Bloomington Stock Center and the Developmental Studies Hybridoma Bank for flies and antibodies.

REFERENCES

1. Artavanis-Tsakonas, S., Rand, M. D., and Lake, R. J. (1999) *Science* **284,** 770–776
2. Fiúza, U. M., and Arias, A. M. (2007) *J. Endocrinol.* **194,** 459–474
3. Moloney, D. J., Panin, V. M., Johnston, S. H., Chen, J., Shao, L., Wilson, R., Wang, Y., Stanley, P., Irvine, K. D., Haltiwanger, R. S., and Vogt, T. F. (2000) *Nature* **406,** 369–375
4. Moloney, D. J., Shair, L. H., Lu, F. M., Xia, J., Locke, R., Matta, K. L., and Haltiwanger, R. S. (2000) *J. Biol. Chem.* **275,** 9604–9611
5. Okajima, T., and Irvine, K. D. (2002) *Cell* **111,** 893–904
6. Brückner, K., Perez, L., Clausen, H., and Cohen, S. (2000) *Nature* **406,** 411–415
7. Haltiwanger, R. S., and Stanley, P. (2002) *Biochim. Biophys. Acta* **1573,** 328–335
8. Okajima, T., Xu, A., Lei, L., and Irvine, K. D. (2005) *Science* **307,** 1599–1603
9. Okajima, T., Reddy, B., Matsuda, T., and Irvine, K. D. (2008) *BMC Biol.* **6,** 1
10. Becker, D. J., and Lowe, J. B. (2003) *Glycobiology* **13,** 41R–53R
11. Roos, C., Kolmer, M., Mattila, P., and Renkonen, R. (2002) *J. Biol. Chem.* **277,** 3168–3175
12. Ishida, N., and Kawakita, M. (2004) *Pflugers Arch.* **447,** 768–775
13. Lühn, K., Wild, M. K., Eckhardt, M., Gerardy-Schahn, R., and Vestweber, D. (2001) *Nat. Genet.* **28,** 69–72
14. Lübke, T., Marquardt, T., Etzioni, A., Hartmann, E., von Figura, K., and Körner, C. (2001) *Nat. Genet.* **28,** 73–76
15. Etzioni, A., Frydman, M., Pollack, S., Avidor, I., Phillips, M. L., Paulson, J. C., and Gershoni-Baruch, R. (1992) *N. Engl. J. Med.* **327,** 1789–1792
16. Hirschberg, C. B. (2001) *J. Clin. Invest.* **108,** 3–6
17. Ishikawa, H. O., Higashi, S., Ayukawa, T., Sasamura, T., Kitagawa, M., Harigaya, K., Aoki, K., Ishida, N., Sanai, Y., and Matsuno, K. (2005) *Proc. Natl. Acad. Sci. U.S.A.* **102,** 18532–18537
18. Hellbusch, C. C., Sperandio, M., Frommhold, D., Yakubenia, S., Wild, M. K., Popovici, D., Vestweber, D., Gröne, H. J., von Figura, K., Lübke, T., and Körner, C. (2007) *J. Biol. Chem.* **282,** 10762–10772
19. Sasamura, T., Ishikawa, H. O., Sasaki, N., Higashi, S., Kanai, M., Nakao, S., Ayukawa, T., Aigaki, T., Noda, K., Miyoshi, E., Taniguchi, N., and Matsuno, K. (2007) *Development* **134,** 1347–1356
20. Aoki, K., Ishida, N., and Kawakita, M. (2003) *J. Biol. Chem.* **278,** 22887–22893
21. Matsuno, K., Ito, M., Hori, K., Miyashita, F., Suzuki, S., Kishi, N., Artavanis-Tsakonas, S., and Okano, H. (2002) *Development* **129,** 1049–1059
22. Persson, U., Izumi, H., Souchelnytskyi, S., Itoh, S., Grimsby, S., Engström, U., Heldin, C. H., Funa, K., and ten Dijke, P. (1998) *FEBS Lett.* **434,** 83–87
23. Takei, Y., Ozawa, Y., Sato, M., Watanabe, A., and Tabata, T. (2004) *Development* **131,** 73–82
24. Ashikov, A., Routier, F., Fuhlrott, J., Helmus, Y., Wild, M., Gerardy-Schahn, R., and Bakker, H. (2005) *J. Biol. Chem.* **280,** 27230–27235
25. Berninsone, P. M., and Hirschberg, C. B. (2000) *Curr. Opin. Struct. Biol.* **10,** 542–547
26. Gerardy-Schahn, R., Oelmann, S., and Bakker, H. (2001) *Biochimie* **83,** 775–782
27. Bakker, H., Routier, F., Oelmann, S., Jordi, W., Lommen, A., Gerardy-Schahn, R., and Bosch, D. (2005) *Glycobiology* **15,** 193–201
28. Nakato, H., Futch, T. A., and Selleck, S. B. (1995) *Development* **121,** 3687–3702
29. David, G., Bai, X. M., Van der Schueren, B., Cassiman, J. J., and Van den Berghe, H. (1992) *J. Cell Biol.* **119,** 961–975
30. Lin, X., and Perrimon, N. (2000) *Matrix Biol.* **19,** 303–307
31. Selleck, S. B. (2001) *Semin. Cell Dev. Biol.* **12,** 127–134
32. Tanimoto, H., Itoh, S., ten Dijke, P., and Tabata, T. (2000) *Mol. Cell* **5,** 59–71
33. Han, C., Belenkaya, T. Y., Khodoun, M., Tauchi, M., Lin, X., and Lin, X. (2004) *Development* **131,** 1563–1575
34. Bornemann, D. J., Duncan, J. E., Staatz, W., Selleck, S., and Warrior, R. (2004) *Development* **131,** 1927–1938
35. Williams, J. A., Paddock, S. W., and Carroll, S. B. (1993) *Development* **117,** 571–584
36. de Celis, J. F., and García-Bellido, A. (1994) *Mech. Dev.* **46,** 109–122
37. Sasamura, T., Sasaki, N., Miyashita, F., Nakao, S., Ishikawa, H. O., Ito, M., Kitagawa, M., Harigaya, K., Spana, E., Bilder, D., Perrimon, N., and Matsuno, K. (2003) *Development* **130,** 4785–4795
38. Acar, M., Jafar-Nejad, H., Takeuchi, H., Rajan, A., Ibrani, D., Rana, N. A., Pan, H., Haltiwanger, R. S., and Bellen, H. J. (2008) *Cell* **132,** 247–258
39. Lühn, K., Laskowska, A., Pielage, J., Klämbt, C., Ipe, U., Vestweber, D., and Wild, M. K. (2004) *Exp. Cell Res.* **301,** 242–250
40. Kochibe, N., and Furukawa, K. (1980) *Biochemistry* **19,** 2841–2846
41. Kurosaka, A., Yano, A., Itoh, N., Kuroda, Y., Nakagawa, T., and Kawasaki, T. (1991) *J. Biol. Chem.* **266,** 4168–4172
42. Luo, Y., and Haltiwanger, R. S. (2005) *J. Biol. Chem.* **280,** 11289–11294
43. Yakubenia, S., Frommhold, D., Schölch, D., Hellbusch, C. C., Körner, C., Petri, B., Jones, C., Ipe, U., Bixel, M. G., Krempien, R., Sperandio, M., and Wild, M. K. (2008) *Blood* **112,** 1472–1481
44. Smith, P. L., Myers, J. T., Rogers, C. E., Zhou, L., Petryniak, B., Becker, D. J., Homeister, J. W., and Lowe, J. B. (2002) *J. Cell Biol.* **158,** 801–815
45. Marquardt, T., Lühn, K., Srikrishna, G., Freeze, H. H., Harms, E., and Vestweber, D. (1999) *Blood* **94,** 3976–3985
46. Hidalgo, A., Ma, S., Peired, A. J., Weiss, L. A., Cunningham-Rundles, C., and Frenette, P. S. (2003) *Blood* **101,** 1705–1712
47. Sturla, L., Rampal, R., Haltiwanger, R. S., Fruscione, F., Etzioni, A., and Tonetti, M. (2003) *J. Biol. Chem.* **278,** 26727–26733